IOP Conf. Series: Materials Science and Engineering **63** (2014) 012109 doi:10.1088/1757-899X/63/1/012109

Influence of the strain rate and deformation temperature on the deformability of Ti-Ni SMAs: A preliminary study

A Kreitcberg[1], S Prokoshkin[2], V Brailovski[3], D Gunderov[4], M Khomutov[5]

[1]PhD Student, National University of Science and Technology "MISiS", Moscow, Russia and Ecole de Technologie Supérieure, Montreal, Canada
[2]Professor, National University of Science and Technology "MISiS", Moscow, Russia
[3] Professor, Ecole de Technologie Supérieure, Montreal, Canada
[4]Leading Researcher, Ufa State Aviation Technical University, Ufa, Russia and Institute of Molecule and Crystal Physics RAS Ufa, Russia
[5]Junior Research Associate, National University of Science and Technology "MISiS", Moscow, Russia
E-mail: alouna87@gmail.com

Abstract. The strain-rate sensitivity of coarse-grained Ti-50.0at.%Ni alloy was studied in the 20 to 500°C temperature range and 10^{-3} to 10^{-5} s^{-1} strain-rate range using the stain-rate jump test. The strain rate sensitivity at a strain rate as low as 10^{-6} s^{-1} was determined using the creep test. A maximum strain-rate-sensitivity exponent m of 0.5 was measured at 500°C in the [10^{-5} –10^{-6}]s^{-1} strain-rate range.

1. Introduction

Ti-Ni shape memory alloys are widely used in both technical and medical fields [1, 2]; improving their functional properties, particularly their fatigue life, is very much an ongoing concern. The formation of a nanocrystalline (NC) structure with 40-60 nm grain size in Ti-Ni alloys has been proven to lead to a three-four times increase in completely recoverable strain and recovery stress, as compared to the coarse-grained (CG) structure [3-8]. A NC structure can be obtained through a two-step thermomechanical treatment (TMT), comprising severe plastic deformation, for example cold rolling (CR), with true strain ε>0.75 followed by post-deformation annealing (PDA) in the 350-450°C temperature range [3, 9, 10]. However, severe plastic deformation-induced defects negatively impact the fatigue life of the Ti-Ni alloy product [4, 11-15]. The improvement of the Ti-Ni alloys deformability is therefore a valuable research objective.

The following parameters should be considered when optimizing the TMT conditions: deformation temperature, strain and strain rate as well as the grain/subgrain size and dislocation density of the initial material. It has been shown [12, 13] that an increase of the rolling temperature up to 150°C and the introduction of intermediate annealing at 400°C (1h) in the TMT schedule lead to both a significant reduction of the processing-induced damage and significant fatigue life improvement of Ti-50.26at.%Ni alloy. However, a higher deformation temperature and intermediate annealing also result in a higher proportion of nanosubgrained (NS) structure at the expense of nanocrystalline (NC) structure, as well as in an overall increase in grain/subgrain size. Determining how to improve the deformability of Ti-Ni alloys, and thereby decrease their processing-induced damageability, while producing truly nanocrystalline Ti-Ni, will make it possible to fully benefit from the fatigue life potential of NC structures.

The deformability of the material, and therefore its resistance to the formation of external and internal defects during plastic deformation, is best determined by the value of the strain-rate-sensitivity exponent, m [16]. Generally, different ranges of m correspond to

different plastic deformation mechanisms, and when superplastic deformation mechanisms (grain boundary sliding at the expense of grain elongation and rotation) prevail, *m* reaches its highest levels of 0.4...0.7 [16, 17].

Normally, superplasticity requires high deformation temperatures and the low strain rates. However, in some extremely fine-grained materials, this effect can be observed at relatively low temperatures and/or relatively high strain rates [18]. It has been shown that the strain-rate sensitivity increases with reduced grain size for FCC structure such as Cu, Al and Ni [19, 20]. For pure Ni at room temperature (RT), for example, a decrease in grain size from 1000 nm to 20 nm leads to an increase in the strain-rate-sensitivity exponent *m* from 0.005 to 0.015 in the $[10^{-1} - 10^{-4}]s^{-1}$ strain-rate range, but at a strain rate lower than 10^{-5} s^{-1}, *m* becomes greater than 0.5 [20-22]. In the case of HCP metals such as Ti, the dependence of *m* on grain size is similar: at RT, in the $[10^{-3} - 10^{-4}]s^{-1}$ strain-rate range, *m* increases from 0.007 to 0.16 when the grain size decreases from 200 μm to 80 nm [23, 24].

The experimental results regarding the grain size, temperature and strain-rate sensitivity of intermetallic compounds, such as Ti-Ni, are limited. Generally, Ti-Ni alloys ductility is studied at elevated temperatures and low strain rates, levels which create favorable conditions for creep in coarse-grained (CG) Ti-Ni alloys. A few studies have used the creep test to calculate the stress exponent *n* and the activation energy *Q* of Dorn's creep equation ($\dot{\varepsilon} = A\sigma^n$) [25], and to identify which deformation mechanism is active at a given temperature. By considering that *n=1/m*, the results of this test can be used to find the strain-rate-sensitivity exponent *m*.

Furthermore, the previous studies have shown that the strain-rate sensitivity of Ti-Ni alloys strongly depends on the deformation temperature and the strain rate, irrespective of the alloys' compositions (near-equatomic or Ni-rich alloys) [26]. For example, the maximum value of $m = 0.5$ was found in CG Ni-rich Ti-Ni alloys in the 470-560°C temperature range for strain rates varying from $2*10^{-9}$ to $8*10^{-6}$ s^{-1} [27, 28]. At higher temperatures (600-1100°C), the highest $m \approx 0.33$-0.37 corresponds to the strain-rate range of $[10^{-3} - 10^{-6}]s^{-1}$, and when the strain rate increases to $[10^{-4} - 10^{-1}]s^{-1}$, *m* decreases to 0.2-0.17 [26, 29-33].

Since most previous studies have been limited to coarse-grained Ti-Ni alloys, low strain rates and high deformation temperatures, extending this study to fine- and ultrafine-grained structures and also to higher strain rates ($>10^{-5}$ s^{-1}) and lower deformation temperatures ($<0.4T_m$) would be a logical progression. This knowledge could be an essential component in determining an appropriate technological window for the production of the damage-free nanocrystalline Ti-Ni alloys.

With this objective in mind, the equal channel angular pressing (ECAP) severe plastic deformation technique represents an interesting alternative to rolling for the creation of favorable microstructure in bulk Ti-Ni alloys. It is known that ECAP with accumulated true strain of $\varepsilon=3.2$ makes it possible to form a fine-grained structure (grain size 450-600 nm) in Ti-Ni alloy, if the material is processed at temperatures of 450°C and higher [34-39], and an ultrafine-grained structure (grain size 200-300 nm), if the material is processed at 400°C.

Thus, our project studies the grain-size, temperature and strain-rate dependences of the strain-rate-sensitivity exponent of Ti-Ni alloys. The results presented here are preliminary and are limited to the coarse-grained Ti-50.0at.%Ni. To validate the proposed methodological approach and to be able to extend it to the fine- and ultrafine-grained Ti-Ni alloys, two concurrent experimental routines (strain-rate-jump testing and creep-testing) and two deformation modes (tension versus plain-strain compression) are evaluated in this work.

2. Experimental

A Ti-50.0at.%Ni alloy was studied. A 19 mm-diameter as-drawn bar supplied by "*Johnson Matthey*" was subjected to homogenizing annealing (800°C, 1h). The martensitic transformation temperatures were measured using a *Perkin-Elmer Pyris* Differential Scanning Calorimeter with a 10°C/min heating-cooling rate.

The mechanical properties were studied using a custom-made tensile machine equipped with a stress-measuring device and a demountable furnace that heated the samples up to 400°C. The tensile samples with working areas of 1×0,25×4,5 mm (Figure 1), were cut from a Ti-50.0at.%Ni bar cross-section and then polished to remove the oxide layer.

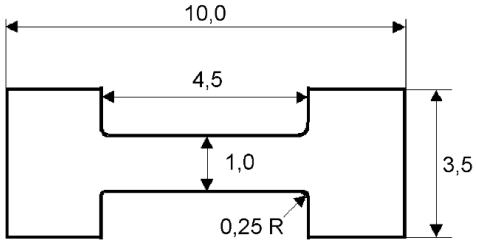

Figure 1 – The geometry of the Ti-50.0at%Ni samples for tensile testing (dimensions in mm)

The strain-rate-jump tensile test [40] was performed at RT, 150, 250 and 400°C with the strain rate ranging from 10^{-3} to 10^{-4} s^{-1}. At the beginning, the sample was deformed with the strain-rate of 10^{-3} s^{-1}. When the flow stress was reached, the strain rate was decreased to 10^{-4} s^{-1}. After reaching a new steady-flow stress, the strain rate was increased again to 10^{-3} s^{-1}. The flow stresses corresponding to the 10^{-3} and 10^{-4} s^{-1} strain rates were measured, and the strain-rate-sensitivity exponent was calculated in conformity with [16]:

$$m = lg\left(\frac{\sigma_2}{\sigma_1}\right) / lg\left(\frac{\dot{\varepsilon}_2}{\dot{\varepsilon}_1}\right) \qquad (1)$$

where m – strain-rate-sensitivity exponent; $\dot{\varepsilon}_1$, $\dot{\varepsilon}_2$ – strain rates, s^{-1}; σ_2, σ_1 – flow stresses at $\dot{\varepsilon}_2$ and $\dot{\varepsilon}_1$.

The strain-rate-jump compressive test was performed using a thermomechanical simulator the *Gleeble System 3800*. The plane strain mode was chosen as being particularly well-suited to the physical simulation of rolling. A series of 20x15x10 mm samples (Figure 2) were cut from the center of the Ti-50.0at.%Ni bar and polished mechanically.

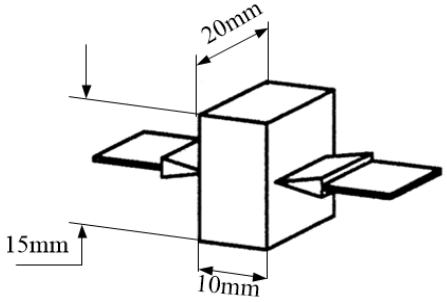

Figure 2 –The geometry of Ti-50.0at%Ni samples for plane-strain testing

The strain-rate-jump compression test was performed at 400 and at 500°C in the [10^{-3} – 10^{-5} s^{-1}] strain-rate range. The samples were heated up to 400 or 500°, then compressed to

a total strain of 15% with a strain rate of 10^{-3} s^{-1} to reach a steady flow. Next, the strain rate was varied from 10^{-3} to 10^{-4} s^{-1} and then from 10^{-4} to 10^{-5} s^{-1} for a total strain of 10%.

Finally, the creep-test was carried out at 400 and 500°C under constant stresses corresponding to 0.4, 0.6, 0.7, 0.8 and $0.9\sigma_y$. The yield stresses σ_y at 400 and 500°C were measured in advance using compression testing up to a total strain of 35% and with a strain rate of 10^{-3} s^{-1}.

The creep curves obtained at different temperatures and under different constant stresses were used to calculate the creep-strain-rates as slopes of the "strain-time" plots. The obtained creep-strain-rates were finally used to determine the strain-rate-sensitivity exponent m as a slope of a $\log(\sigma)$ vs $\log(\dot{\varepsilon})$ plot, where σ are the creep-test constant stresses and $\dot{\varepsilon}$ are the corresponding strain rates) [32].

3. Experimental Results

3.1 Microstructure

The results of the metallographic analysis of the quenched Ti-50.0 at.% Ni alloy show that the average B2-austenite grain size is 200-300 μm (Figure 3a). As can be observed from the X-ray diffractogram and the DSC plot (Figure 3b,c), at room temperature, the alloy is almost completely martensitic with less than 5% of B2-austenite retained. The determined by X-ray martensitic transformation temperatures correspond to A_f = 98°C and M_f = 20°C, thus corroborating the DSC results.

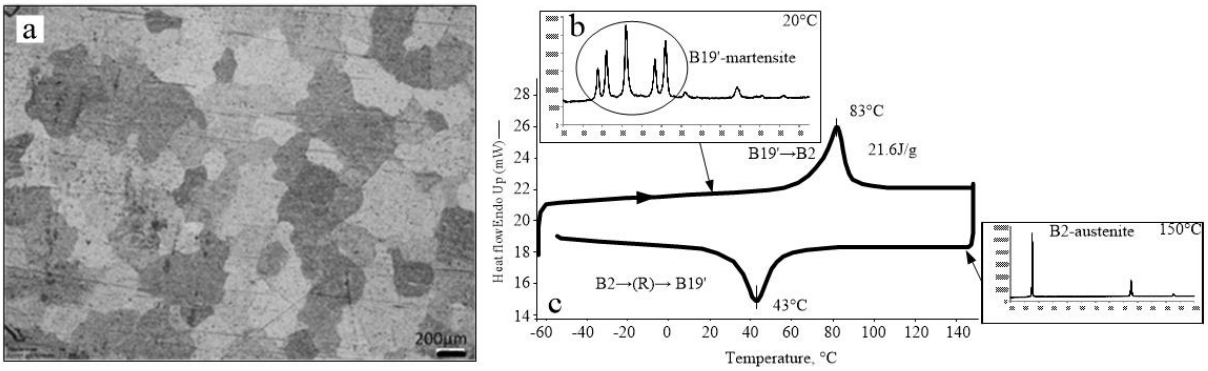

Figure 3 – Structure and transformations of Ti-50.0 at.%Ni alloy after quenching from 800°C, 1h, a – optical metallography, b – X-ray diffractogram, c – DSC plot

3.2 Strain-rate-sensitivity exponent

The strain-rate-sensitivity exponent m was measured at different temperatures (RT, 150, 250 and 400°C) in the $[10^{-3} – 10^{-4}]s^{-1}$ strain-rate range using the strain-rate-jump tensile test. The stress-strain curves of the strain-rate-jump test are shown in Figure 4. The strain-rate-sensitivity exponents calculated using Eq. 1 are collected in Table 1.

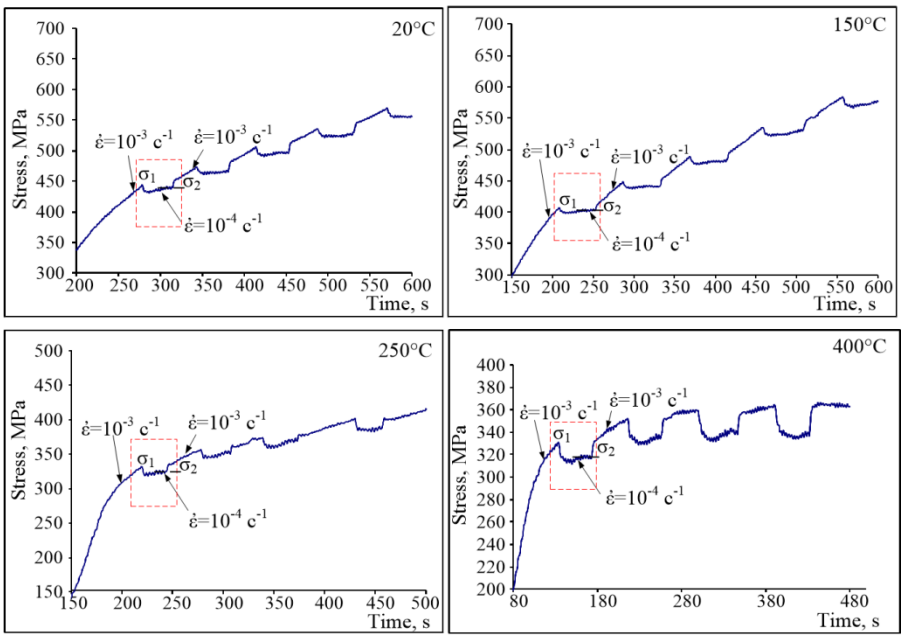

Figure 4 – The stress-strain curves of the strain-rate-jump test at different temperatures

Table 1 – The results of the strain-rate sensitivity measurements using the strain-rate-jump tensile test

Temperature, °C	*m*
20	0.006±0.001
150	0.006±0.002
250	0.012±0.006
400	0.028±0.005

By evaluating the results collected in Table 1, it can be stated that the stain-rate-sensitivity exponent *m* increases from 0.006 to 0.028 when the testing temperature rises from RT to 400°C. However, the exponent *m* remain too low as compared to the superplasticity-relevant values of about 0.5, throughout the entire range of temperatures (20 - 400°C) and strain rates [10^{-3} – 10^{-4} s^{-1}]. These low values mean that the testing temperature should be increased and/or the strain rate decreased to eventually reach superplasticity [16, 17].

Since the tensile testing machine did not allow the strain rate to be sufficiently lowered, the strain-rate-jump test was repeated in compression plane-strain mode. At 400°C, the tests were carried out in the [10^{-4} – 10^{-5}]s^{-1} strain-rate range, while at 500°C, in the strain-rate range of [10^{-3} – 10^{-4}] and [10^{-4} – 10^{-5}]s^{-1}. The results are presented in Figure 5.

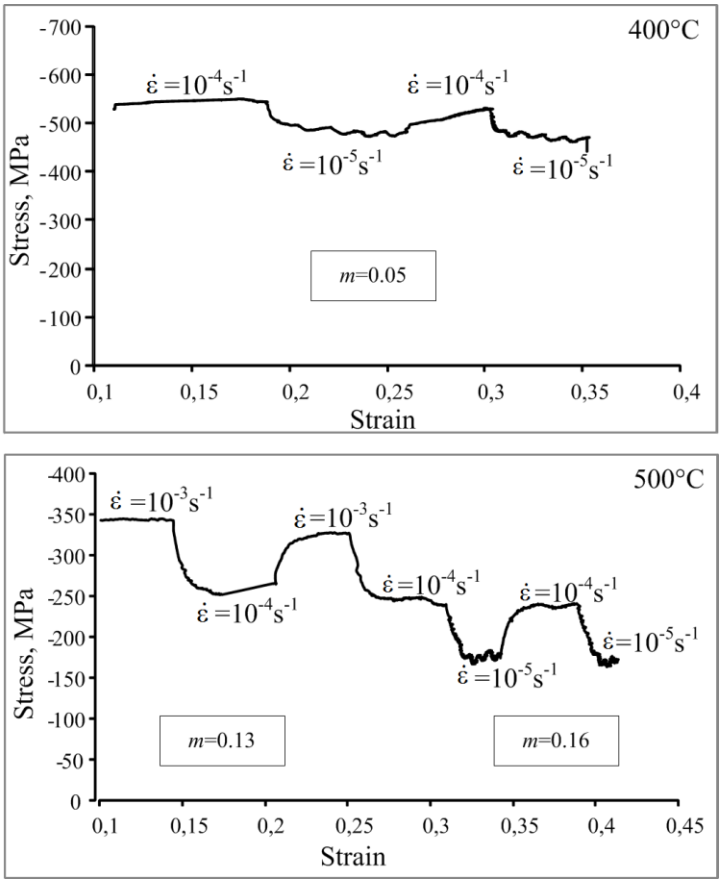

Figure 5 – The strain-rate-jump tests in compression plain-stress mode at 400 and at 500°C

At 400°C, the strain-rate-sensitivity exponent corresponds to 0.05 at $[10^{-4} – 10^{-5}]s^{-1}$. When the test temperature was raised to 500°C, m = 0.13 $[10^{-3} – 10^{-4}]s^{-1}$ and m= 0.15 $[10^{-4} – 10^{-5}]s^{-1}$. Thus, the highest measured value of $m = 0.15$ (at 500°C and $[10^{-4}$ and $10^{-5}]s^{-1}$) remains too low to make a conclusion about the superplasticity of CG Ti-50.0at.%Ni alloy.

As an alternative, the creep test can be useful to determine m values at low strain rates. This test reduces the effects of machine rigidity and system inertia. The classical equation for creep test is:

$$\sigma = A \cdot \dot{\varepsilon}^{m}$$

where m is the strain-rate-sensitivity exponent, and $\dot{\varepsilon}$ is the strain rate under constant stress σ.

The stress-strain compression diagrams obtained with a strain rate of 10^{-3} s^{-1} at 400 and 500°C are shown in Figure 6. The yield stresses correspond to 320 MPa at 400°C and 208 MPa at 500°C. The strain-rate sensitivity was measured at 400 and 500°C under constant stresses corresponding to 0.4, 0.6, 07, 0.8 and 0.9-0.95σ_y, i.e. 192, 224, 256, 288 and 304 MPa at 400°C and 83, 125, 146, 166 and 187 MPa at 500°C. The resulting creep curves are presented in Figure 7.

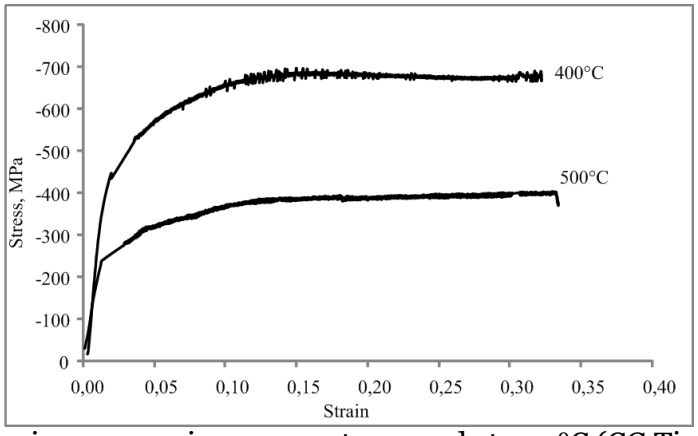

Figure 6 - Stress-strain compression curves at 400 and at 500°C (CG Ti-50.0at.%Ni)

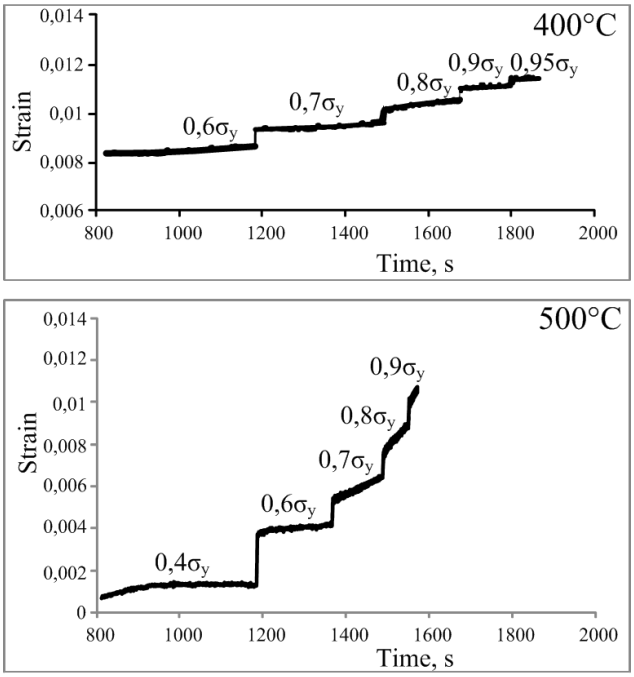

Figure 7 – Creep curves under different constant stresses at 400 and at 500°C (CG Ti-50.0 at.%Ni)

The creep strain rates at 400 and 500°C were determined as slopes of the "strain vs time" plots for each of the applied stresses. For 400°C and $0.4\sigma_y$ (192 MPa), the creep-strain rate was too low to be measured. For $0.6\sigma_y$ (224 MPa), the creep-strain rate corresponds to $1.4*10^{-6}$ s^{-1}. When the stress was raised to $0.95\sigma_y$ (304 MPA), the strain rate increased to $9.6*10^{-6}$ s^{-1}.

The creep-strain rates at 400°C therefore increases from $1.4*10^{-6}$ (192 MPa) to $9.6*10^{-6}$ s^{-1} (304 MPa). When the testing temperature was increased to 500°C, the creep strain rate increases from $2*10^{-6}$ (83 MPa) to $4*10^{-5}$ s^{-1} (187 MPa). These data were used to calculate the strain-rate sensitivity exponent as a function of both strain rate and stress. The results are presented in Figure 8.

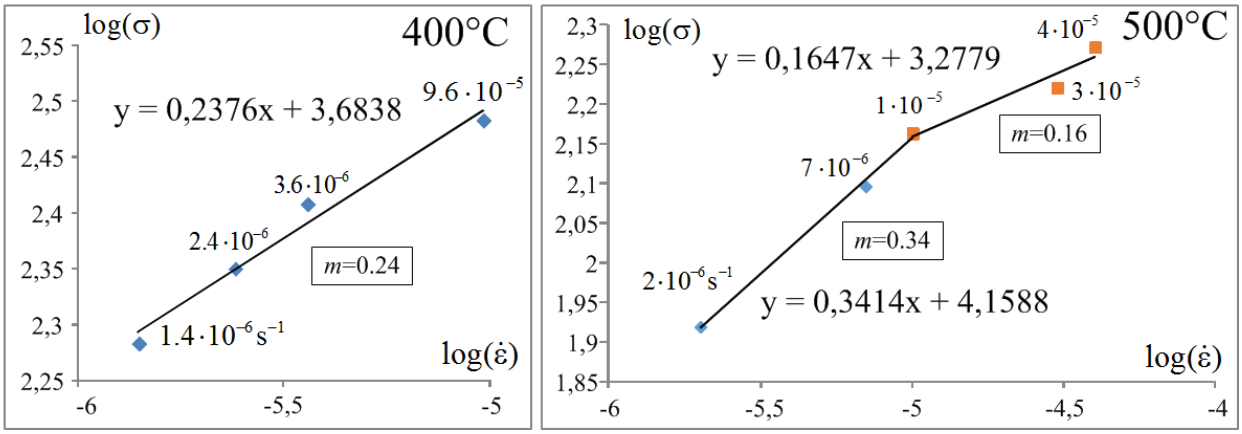

Figure 8 – The log(σ) vs log($\dot{\varepsilon}$) plots at 400 and 500°C

According to Figure 8, at 400°C, m ≈ 0.24 for the [10^{-5} - 10^{-6}]s^{-1} strain-rate range. At 500°C, the creep plot splits into two parts corresponding to two strain-rate ranges: [10^{-6} – 10^{-5}] and [10^{-5} – 10^{-4}]s^{-1}. Thus, m = 0.16 for the [10^{-4} and 10^{-5}]s^{-1} strain-rate range and 0.34 for the [10^{-5} and 10^{-6}]s^{-1} strain-rate range. Note that the results obtained for the same [10^{-4} and 10^{-5}]s^{-1} strain-rate range using the strain-rate-jump compression test and using the creep-test are comparable (m = 0.15 for the first and m = 0.16, for the second).

4. Discussion

After homogenizing annealing at 800°C (1h), Ti-50.0at.%Ni alloy has a martensitic structure at room temperature with an average grain size of 200-300μm. The strain-rate sensitivity of CG Ti-50.0at.%Ni alloy was measured in the [10^{-3} and 10^{-6}]s^{-1} strain-rate range at 20 and 150°C (B19'-martensite), and at 250, 400 and 500°C (B2-austenite). The results showed that for the strain-rate range [10^{-3} and 10^{-4}]s^{-1}, strain-rate sensitivity at 20 and 150°C is very week: m=0.006. For the same strain-rate range, the higher the temperature, the greater the strain-rate sensitivity; and a slower progression m = 0.012 (250°C) and 0.03 (400°C) is followed by a step-wise rise: m= 0.13 (500°C).

A decrease in the strain-rate range from [10^{-3} – 10^{-4}] to [10^{-4} – 10^{-5}]s^{-1} and then to [10^{-5} – 10^{-6}]s^{-1} leads to a further increase of m. The highest strain-rate sensitivities are obtained in the [10^{-5} – 10^{-6}]s^{-1} strain-rate range: m = 0.24 (400°C) and m = 0.34 (500°C) (Figure 9).

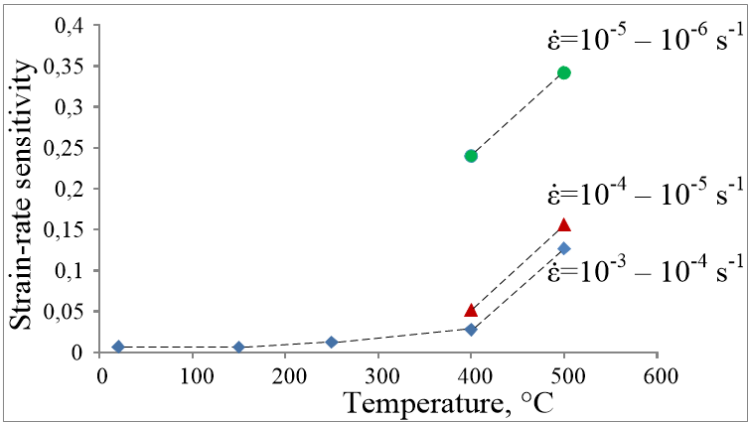

Figure 9 – The strain-rate sensitivity of Ti-50.0at.%Ni alloy as a function of temperature

According to the literature, the superplasticity mechanisms prevail when the strain-rate-sensitivity exponent m varies between 0.4 – 0.7 [16, 17]. In this work on the CG Ti-50.0at.%Ni alloy, the maximum strain-rate sensitivity exponent obtained, m=0.34, is close to the lower limit of this range.

Since the strain-rate sensitivity is grain-size-dependent, we can reasonably expect that the strain-rate sensitivity will increase if the alloy's grain size decreases [19-21, 23, 24]. Therefore, for further work, the grain size of Ti-50.0at.%Ni alloy will be refined using the equal channel angular pressing (ECAP) technique, and the study will be repeated using the experimental routines validated in the framework of this preliminary study: tension/compression strain-rate-jump testing, and compression-creep testing (see Figure 10).

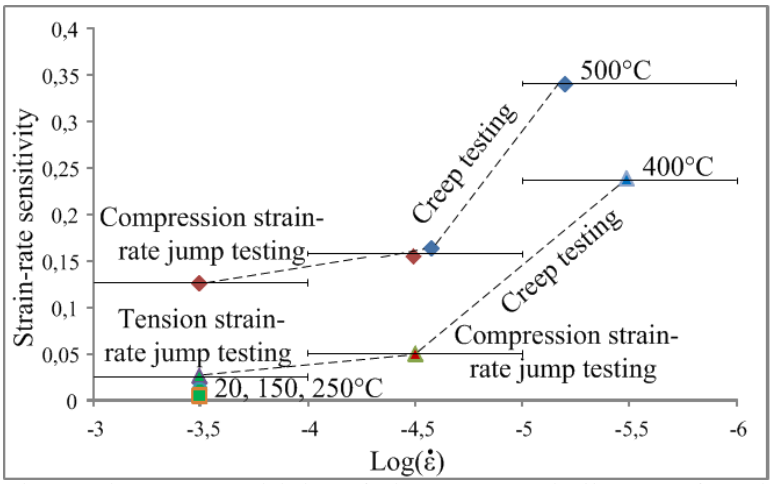

Figure 10 – The strain-rate sensitivity of Ti-50.0at.%Ni alloy as a function of strain rate

5. Conclusions

1. For the coarse-grained Ti-50.0at.%Ni alloy, the maximum value of the strain-rate sensitivity exponent m = 0.34 was obtained in the case of deformation at 500°C in the strain rate range from 10^{-5} to 10^{-6} s^{-1}. The smaller m value (0.24) was measured in the case of deformation at 400°C in the same strain-rate range.

2. A comparison of the results of compression/tension strain-rate-jump testing with creep-testing showed a good convergence of the measured strain-rate sensitivity exponent values.

Acknowledgements

The authors are grateful to the Natural Sciences and Engineering Research Council of Canada and to the Ministry of Education and Science of the Russian Federation for their financial support.

6. References

[1] K. Otsuka, and C. M. Wayman 1998 Shape memory materials (Cambridge University Press, United Kingdom).

[2] T. W. Duerig, K. N. Melton, D. Stockel et al. 1990 Engineering aspects of shape memory alloys (Butterworth-Heinemann. London).
[3] V. Brailovski, K. Inaekyan, S. Prokoshkin et al. 2007 Structure and properties features of nanostructured Ti-Ni SMA after severe plastic deformation and post-deformation annealing *Proc. Int. Conf. on Shape Memory and Superelastic Technologies (SMST-2007)* p. 17-26.
[4] V. Brailovski, S. Prokoshkin, K. Inaekyan et al. 2011 Functional properties of nanocrystalline, submicrocrystalline and polygonized Ti-Ni alloys processed by cold rolling and post-deformation annealing *Journal of Alloys and Compounds* vol. 509, no. 5, pp. 2066-2075.
[5] V. Brailovski, S. D. Prokoshkin, I. Y. Khmelevskaya et al. 2006 Structure and properties of the Ti-50.0 at% Ni alloy after strain hardening and nanocrystallizing thermomechanical processing *Materials Transactions* vol. 47, no. 3, pp. 795-804.
[6] N. N. Kuranova, D. V. Gunderov, A. N. Uksusnikov et al. 2009 Effect of heat treatment on the structural and phase transformations and mechanical properties of TiNi alloy subjected to severe plastic deformation by torsion *Physics of Metals and Metallography* vol. 108, no. 6, pp. 556-568.
[7] A. V. Sergueeva, C. Song, R. Z. Valiev et al. 2003 Structure and properties of amorphous and nanocrystalline NiTi prepared by severe plastic deformation and annealing *Materials Science and Engineering A* vol. A339, no. 1-2, pp. 159-65.
[8] K. Tsuchiya, M. Ohnuma, K. Nakajima et al. 2009 Microstructures and enhanced properties of SPD-processed TiNi shape memory alloy *Materials and Devices for Smart Systems III*. pp. 113-24.
[9] S. D. Prokoshkin, V. Brailovski, K. E. Inaekyan et al. 2008 Structure and properties of severely cold-rolled and annealed Ti-Ni shape memory alloys *Materials Science and Engineering A* vol. 481-482, pp. 114-18.
[10] S. D. Prokoshkin, V. Brailovskii, I. Y. Khmelevskaya et al. 2005 Creation of substructure and nanostructure in thermomechanical treatment and control of properties of Ti-Ni alloys with shape memory effect *Metal Science and Heat Treatment* vol. 47, no. 5-6, pp. 182-7.
[11] V. Demers, V. Brailovski, S. D. Prokoshkin et al. 2009 Thermomechanical fatigue of nanostructured Ti-Ni shape memory alloys *Materials Science and Engineering A* vol. 513-514, no. 1-7, pp. 185-96.
[12] Y. Facchinello, V. Brailovski, K. Inaekyan et al. 2013 Manufacturing of monolithic superelastic rods with variable properties for spinal correction: Feasibility study *Journal of the Mechanical Behavior of Biomedical Materials* vol. 22, pp. 1-11.
[13] A. Kreitcberg, V. Brailovski, S. Prokoshkin et al. 2013 Microstructure and functional fatigue of nanostructured Ti-50.26at%Ni alloy after thermomechanical treatment with warm rolling and intermediate annealing *Materials Science and Engineering A* vol. 562, pp. 118-127.
[14] S. Miyazaki, K. Mizukoshi, T. Ueki et al. 1999 Fatigue life of Ti-50 at.% Ni and Ti-40Ni-10Cu (at.%) shape memory alloy wires *Material Science and Engineering A* pp. 658-63.
[15] A. Kreitcberg, V. Brailovski, S. Prokoshkin et al. 2014 Influence of thermomechanical treatment on structure and crack propagation in nanostructured Ti-50.26 at%Ni alloy *Metallography, Microstructure, and Analysis* vol. 3, p. 46-57.
[16] A. K. Mukherjee, and R. S. Mishra 2001 Superplasticity, *Encyclopedia of materials: Science and Thechnology* no. 2, pp. 8977-8981.
[17] A. K. Mukherjee 2002 An examination of the constitutive equation for elevated temperature plasticity *Material Science and Engineering A* pp. 1-22.
[18] M. J. Mayo 1997 High and low temperature superplasticity in nanocrystalline materials *Nanostructuctured Materials* vol. 9, pp. 717-26.

[19] Q. Wei 2007 Strain rate effects in the ultrafine grain and nanocrystalline regimes nfluence on some constitutive responses *Journal of Materials Science* vol. 42, no. 5, pp. 1709-27.
[20] Q. Wei, S. Cheng, K. T. Ramesh et al. 2004 Effect of nanocrystalline and ultrafine grain sizes on the strain rate sensitivity and activation volume: Fcc versus bcc metals *Materials Science and Engineering A* vol. 381, no. 1-2, pp. 71-79.
[21] N. Wang, Z. Wang, K. T. Aust et al. 1997 Room temperature creep behavior of nanocrystalline nickel produced by an electrodeposition technique *Materials Science and Engineering A* vol. A237, no. 2, pp. 150-158.
[22] R. Schwaiger, B. Moser, M. Dao et al. 2003 Some critical experiments on the strain-rate sensitivity of nanocrystalline nickel *Acta Materialia* vol. 51, no. 17, pp. 5159-5172.
[23] F. Wang, B. Li, T. T. Gao et al. 2013 Activation volume and strain rate sensitivity in plastic deformation of nanocrystalline Ti *Surface and Coatings Technology* vol. 228, no. SUPPL.1, pp. S254-S256.
[24] X. Liu, X. Zhao, and X. Yang 2011 Strain rate sensitivity of ultrafine-grained CP-Ti processed by ECAP at room temperature *Materials Science Forum* pp. 707-712.
[25] J. E. Dorn 1955 Some fundamental experiments on high temperature creep *Journal of the Mechanics and Physics of Solids* vol. 3, no. 2, pp. 85-116.
[26] H. Kato, T. Yamamoto, S. Hashimoto et al. 1999 High-temperature plasticity of the -phase in nearly-equiatomic nickel-titanium alloys *Materials Transactions* vol. 40, no. 4, pp. 343-50.
[27] G. Eggeler, J. Khalil-Allafi, K. Neuking et al. 2002 Creep of binary Ni-rich NiTi shape memory alloys and the influence of pre-creep on martensitic transformations *Zeitschrift fur Metallkunde* vol. 93, no. 7, pp. 654-60.
[28] E. Kobus, K. Neuking, G. Eggeler et al. 2002 The creep behaviour of a NiTi-alloy and the effect of creep deformation on it's shape memory properties *Praktische Metallographie* vol. 39, no. 4, pp. 177-86.
[29] S.-Y. Jiang, Y.-Q. Zhang, and Y.-N. Zhao 2013 Dynamic recovery and dynamic recrystallization of NiTi shape memory alloy under hot compression deformation *Transactions of Nonferrous Metals Society of China (English Edition)* vol. 23, no. 1, pp. 140-147.
[30] M. Morakabati, M. Aboutalebi, S. Kheirandish et al. 2011 High temperature deformation and processing map of a NiTi intermetallic alloy *Intermetallics* vol. 19, no. 10, pp. 1399-1404.
[31] C. Lexcellent, P. Robinet, J. Bernardini et al. 2005 High temperature creep measurements in equiatomic Ni-Ti shape memory alloy *Materialwissenschaft und Werkstofftechnik* pp. 509-512.
[32] A. K. Mukherjee 1968 High-temperature-creep mechanism of TiNi *Symposium on TiNi and Associated Compounds* pp. 2201-2204.
[33] S. M. Oppenheimer, A. R. Yung, and D. C. Dunand 2007 Power-law creep in near-equiatomic nickel-titanium alloys *Scripta Materialia* vol. 57, no. 5, pp. 377-80.
[34] V. V. Stolyarov, E. A. Prokof'ev, S. D. Prokoshkin et al. 2005 Structural features, mechanical properties, and the shape-memory effect in TiNi alloys subjected to equal-channel angular pressing *Physics of Metals and Metallography* vol. 100, no. 6, pp. 608-18.
[35] V. G. Pushin, D. V. Gunderov, N. I. Kourov et al. 2004 Nanostructures and phase transformations in TiNi shape memory alloys subjected to severe plastic deformation *Ultrafine Grained Materials 3 Symposium* pp. 481-6.
[36] V. G. Pushin, V. V. Stolyarov, R. Z. Valiev et al. 2005 Nanostructured TiNi-based shape memory alloys processed by severe plastic deformation *Materials Science and Engineering A* vol. 410-411, pp. 386-389.

[37] V. G. Pushin, and R. Z. Valiev 2003 The nanostructured TiNi shape-memory alloys: New properties and applications *Diffusion and Defect Data Pt.B: Solid State Phenomena* pp. 13-24.
[38] N. N. Popov, A. I. Korshunov, A. A. Aushev et al. 2006 Effect of nanostructurizing and rate of inducing deformation on the structural and thermomechanical characteristics of a titanium nickelide-based alloy *Physics of Metals and Metallography* vol. 102, no. 4, pp. 432-8.
[39] Z. Fan, and C. Xie 2008 Phase transformation behaviors of Ti-50.9at.% Ni alloy after Equal Channel Angular Extrusion *Materials Letters* vol. 62, no. 6-7, pp. 800-803.
[40] Y. M. Haddad 2001 Mechanical behaviour of engineering materials *Kluwer Academic Publishers*.